THE JOURNAL OF BIOLOGICAL CHEMISTRY VOL. 286, NO. 36, pp. 31915–31923, September 9, 2011

Glycosylation Increases the Thermostability of Human Aquaporin 10 Protein*[S]

Received for publication, March 23, 2011, and in revised form, July 6, 2011 Published, JBC Papers in Press, July 6, 2011, DOI 10.1074/jbc.M111.242677

Fredrik Öberg[‡], Jennie Sjöhamn[‡], Gerhard Fischer[‡], Andreas Moberg[‡], Anders Pedersen[§], Richard Neutze[‡], and Kristina Hedfalk[‡1]

From the [‡]Department of Chemistry/Biochemistry, University of Gothenburg, P. O. Box 462, SE-405 30 Göteborg, Sweden and the [§]Swedish NMR Centre, University of Gothenburg, P. O. Box 465, SE-405 30 Göteborg, Sweden

Human aquaporin10 (hAQP10) is a transmembrane facilitator of both water and glycerol transport in the small intestine. This aquaglyceroporin is located in the apical membrane of enterocytes and is believed to contribute to the passage of water and glycerol through these intestinal absorptive cells. Here we overproduced hAQP10 in the yeast *Pichia pastoris* and observed that the protein is glycosylated at Asn-133 in the extracellular loop C. This finding confirms one of three predicted glycosylation sites for hAQP10, and its glycosylation is unique for the human aquaporins overproduced in this host. Nonglycosylated protein was isolated using both glycan affinity chromatography and through mutating asparagine 133 to a glutamine. All three forms of hAQP10 where found to facilitate the transport of water, glycerol, erythritol, and xylitol, and glycosylation had little effect on functionality. In contrast, glycosylated hAQP10 showed increased thermostability of 3–6 °C compared with the nonglycosylated protein, suggesting a stabilizing effect of the *N*-linked glycan. Because only one third of hAQP10 was glycosylated yet the thermostability titration was mono-modal, we suggest that the presence of at least one glycosylated protein within each tetramer is sufficient to convey an enhanced structural stability to the remaining hAQP10 protomers of the tetramer.

Intrinsic membrane proteins are essential for the selective transport of molecules in and out of cells and hence the regulation of their concentration within the cell. Aquaporins (AQPs)[2] primarily facilitate the transport of water across biological membranes, where water movements are driven by hypertonic or hypotonic conditions. AQPs consist of six transmembrane domains and five connecting loops (Fig. 1) with both termini located on the intracellular side of the membrane. Aquaporins also contain two half-helices in loops B and E which align to form a pseudo-transmembrane helix, the focus of which contains the signature motif asparagine-proline-alanine (NPA). *In vivo* the protein assemblies into homotetramers, and each monomer functions as a water channel. Thirteen aquaporin family members exist within humans, with varying tissue distribution and substrate specificity (1). Two major subclasses have been identified: the orthodox aquaporins (hAQP0, hAQP1, hAQP2, hAQP4, hAQP5, hAQP6, and hAQP8) mainly facilitating the movement of water, and the aquaglyceroporins (hAQP3, hAQP7, hAQP9, and hAQP10) which facilitate both the transport of water and of other small solutes.

Human aquaporin10 (hAQP10) was first identified in a human jejunum cDNA library and was observed to have 264 amino acids and dual copies of the aquaporin signature NPA motifs, confirming it as a member of the aquaporin family located in the small intestine (2). From homology studies the protein had been classified as an aquaglyceroporin, but surprisingly it did not show any glycerol or urea transport and only a low permeability to water in *Xenopus* oocytes (2). Shortly thereafter, an independent study identified a 301-amino acid protein with a different sixth transmembrane domain which transported both glycerol and water in *Xenopus* oocytes (3). From this observation it was concluded that the former assignment corresponded to an incomplete splice version where an insert of 475 nucleotides causes a frameshift and a different termination resulting in a shorter and nonfunctional protein. Both studies, nevertheless, placed the protein in the small intestine (4), and later work considering the subcellular distribution of hAQP10 placed it in the apical membrane of absorptive intestinal epithelial cells, where it can facilitate the flow of water and other small molecules from the intestinal lumen (5).

Glycosylation is the most common form of posttranslational modification in eukaryotes (6), and from analysis of the Protein Sequence Data Bank, a majority of all proteins are thought to be glycoproteins (7). A glycan (also referred to as carbohydrate or saccharide) is attached to certain secreted proteins and membrane proteins when passing through the secretory pathway. There are two major types of protein-saccharide linkages found in eukaryotic glycoproteins, and these are commonly referred to as *N*-linked and *O*-linked glycosylation because the glycosylation occurs via covalent bonds to a nitrogen and oxygen, respectively. *N*-Linked glycosylation occurs co-translationally in the endoplasmatic reticulum (ER) where the lipid-linked glycan precursor, initially anchored to the ER membrane, is transferred to an asparagine residue in an Asn-*X*-Ser/Thr recognition sequence called a sequon, where *X* can be any amino acid except a proline (8). Processing of the glycan occurs already in

* This work was supported by the Swedish Science Research Council, the European Commission Marie Curie Training Network Aquaglyceroporins, and the Integrated Project EDICT.

[S] The on-line version of this article (available at http://www.jbc.org) contains supplemental Tables S1–S4, Figs. S1–S3, Experimental Procedures, and additional references.

[1] To whom correspondence should be addressed. Tel.: 46-31-786-3923; Fax: 46-31-786-3910; E-mail: kristina.hedfalk@chem.gu.se.

[2] The abbreviations used are: AQP, aquaporin; DDM, *n*-dodecyl-β-D-maltopyranoside; ER, endoplasmatic reticulum; $Man_8GlcNAc_2$, *N*-acetylglucosamine$_2$mannose$_8$; NPA, asparagine-proline-alanine motif; Pf, osmotic water permeability; PNGase F, peptide-*N*-glycosidase F; SPR, surface plasmon resonance; T_m, melting temperature.

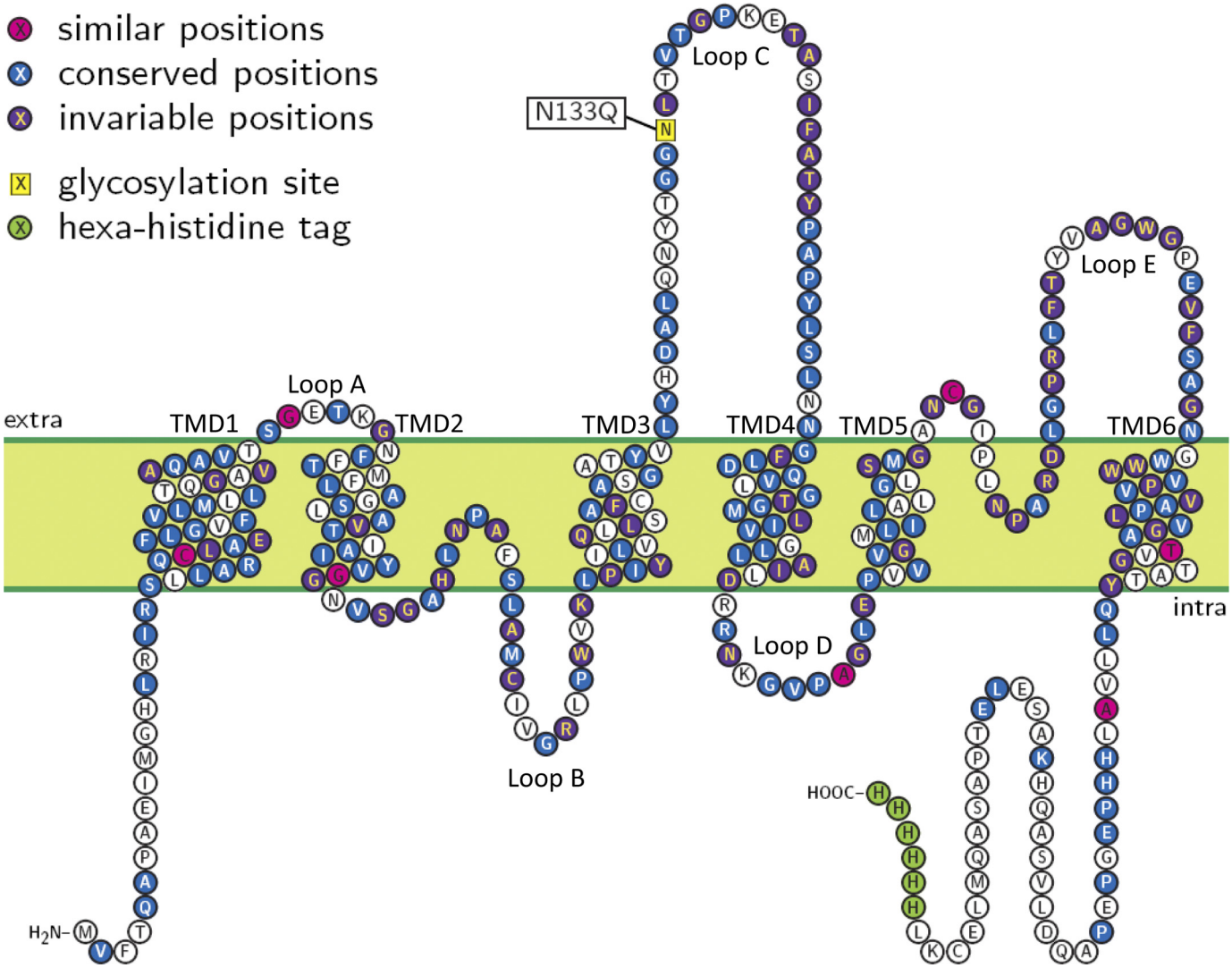

FIGURE 1. **Snake plot of hAQP10 compared with the other human aquaglyceroporins (hAQP3, hAQP7, and hAQP9).** Similar residues are shown in *red*, conserved in *blue*, and invariable in *purple* (as indicated by a dot (.), a colon (:), and a star (*) when aligning the sequences using the ClustalW tool). The glycosylation site that was mutated in hAQP10 has been marked as well as the histidine tag.

the ER lumen before the protein has been fully synthesized and folded (9), and the protein is subsequently transported to the Golgi apparatus where it is further processed (10) before being localized to its cellular destination. A mammalian cell can build a glycan in a vast number of ways, making glycosylation the most diverse of all posttranslational modifications.

The initial glycosylation processes are very similar in the yeast ER compared with the mammalian one. However, the processing of the glycan in the Golgi apparatus is completely different in yeast, and it often results in a core complex composed of *N*-acetylglucosamine$_2$mannose$_8$ ($Man_8GlcNAc_2$) or $Man_9GlcNAc_2$, even though this may differ between different yeast species (11). *Saccharomyces cerevisiae* usually adds a large number of residues to this core, giving a final glycan with more than 100 mannose residues (12). In *Pichia pastoris* the glycans are generally shorter, ranging between 8 and 14 mannose residues (13, 14).

Glycosylated proteins have been studied for decades, and multiple roles have been suggested to be of relevance for many processes and functions, including protein folding and stability, transport of proteins through the secretory pathways, molecular recognition processes, and cell-cell interaction (15). When a protein has been synthesized in the polarized intestinal epithelial cells, signals will direct it to the apical domain or the basolateral domain. Such a signal could be an attached *N*-linked glycan (16, 17), implying that the glycan is important for the protein to be correctly sorted. In several cases the removal of a glycan has been observed to decrease the function, production level, and/or stability of the protein. This may be due to the protein being less stable, which will cause it to be more rapidly degraded in the cell, or due to improper folding resulting in protein aggregation and precipitation (18–21). Thermodynamic stabilization calculations suggest that the covalent binding of a glycan to a protein surface may enhance the thermal stability of the protein, which can be measured as an increase in melting temperature (22). Perhaps unexpectedly, the same study showed that the length of each glycan had only a minor effect on the degree of stabilization (22).

In this work we characterize hAQP10 overproduced in *P. pastoris* and demonstrate that this aquaporin transports water

as well as short chain and medium chain sugar alcohols. Moreover we observe that *N*-linked glycosylation occurs for a defined population of the purified hAQP10, which was identified using both staining and mass spectrometry. Glycosylated and nonglycosylated hAQP10 were separated using a glycan affinity chromatography and by engineering a hAQP10 mutant lacking the glycan. From comparison of the thermostability of these different proteins using circular dichroism spectroscopy, we observe a shift of 3–6 °C upon the addition of the glycan and argue that this enhanced stability for the glycosylated protein is conveyed through a cooperative mechanism to all aquaporins within the hAQP10 tetramer.

EXPERIMENTAL PROCEDURES

Cloning, Protein Production, Solubilization, and Purification of hAQP10 from P. pastoris—The recombinant *P. pastoris* strain used in this study has been described earlier (23). hAQP10 in *P. pastoris* was cultivated in a 3l-fermentor (Infors-HT) following the general guidelines from Invitrogen (24) and as described in a previous study on hAQP1 (25). The expression of recombinant hAQP10 was induced by a simultaneous mixed feed containing equal amounts of 40% methanol and 60% sorbitol, respectively, as an alternative to only using methanol to improve induction during the membrane protein production phase.

A 30-g cell pellet was resuspended in 20 ml of breaking buffer (50 mM potassium phosphate buffer, pH 7.5, 5% glycerol) and disrupted by three passages through an X-press cell. Cell debris was collected by centrifugation at 10,000 × *g* for 20 min and 15,000 × *g* for 30 min at 4 °C. Membranes were collected and washed with 4 M urea by centrifugation at 158,000 × *g* for 90 min at 4 °C. The resulting membrane pellet was resuspended in 7 ml of membrane resuspension buffer (20 mM HEPES, pH 7.8, 50 mM NaCl, 10% glycerol, 2 mM β-mercaptoethanol) per g of membrane pellet.

10 ml of solubilization buffer (membrane resuspension buffer with 2% *n*-dodecyl-β-D-maltopyranoside (DDM), Affymetrix) was added to an equal volume of membrane solution and left for stirring for 3 h at 4 °C. Nonsolubilized material was removed by centrifugation at 140,000 × *g* for 30 min at 4 °C, and the resulting supernatant was incubated with 1 ml nickel-nitrilotriacetic acid slurry (Qiagen) overnight at 4 °C. The supernatant representing the nonbound fraction was removed, and the resin was washed and transferred to a gravity flow column where it was eluted with elution buffer (20 mM HEPES, pH 7.8, 300 mM NaCl, 10% glycerol, 2 mM β-mercaptoethanol, 0.02% DDM, and 300 mM imidazole). Fractions containing hAQP10 were collected and concentrated (Vivaspin 100,000 MWCO) before injection on a size exclusion chromatography column (Superdex200; GE Healthcare) and eluted with gel filtration buffer (20 mM Tris-HCl, pH 7.5, 100 mM NaCl, 0.02% DDM). Fractions were analyzed on SDS-PAGE, and fractions from the peak were concentrated to a final concentration around 10 mg/ml in a 100,000 MWCO concentrator tube (Vivaspin).

A HiTrap Con A 4B (prepacked with concanavalin A-Sepharose 4B) affinity column (GE Healthcare) was used for purification of hAQP10-ΔGlyc. First, the heterogeneous hAQP10 sample from the nickel-nitrilotriacetic acid purification was loaded onto a PD10 column (GE Healthcare), and to exchange the buffer it was eluted with binding buffer (20 mM Tris-HCl, pH 7.4, 0.5 M NaCl, 1 mM $MnCl_2$, 1 mM $CaCl_2$, 0.02% DDM). Subsequently, the sample was loaded onto the Sepharose 4B column. Due to interactions between lectin and detergent, all protein was bound to the column, and the hAQP10-ΔGlyc fraction was obtained in elution buffer (20 mM Tris-HCl, pH 7.4, 0.5 M NaCl, 0.5 M methyl α-D-glucopyranoside, 0.02% DDM). The glycosylated fraction remained tightly bound to the column.

Glycosylation Studies—A Pro-Q Emerald 488 Glycoprotein Gel kit (P21875; Invitrogen) was used to stain purified protein analyzed on a SDS-PAGE. The protein was fixed to the gel by addition of fixing solution and incubation overnight followed by a washing step in wash solution for 2 × 15 min. To oxidize the carbohydrates the gel was incubated in 25 ml of oxidizing solution for 20 min and washed for 3 × 15 min in the wash solution. Staining of the gel was done in the dark with 25 ml of Pro-Q Emerald 488 Staining solution for 2 h. Subsequently, the gel was washed in 100 ml of wash solution for 3 × 30 min followed by imaging with excitation at 400 nm and emission at 530 nm. After imaging with the glycostain, the gel was rinsed in water for 2 × 5 min, and 60 ml of SYPRO Ruby Protein Gel stain (Invitrogen) was added to stain all proteins. During a total staining time of 30 min the gel was heated to ~80 °C for 3 × 30 s. Finally, the gel was washed with wash solution and mQ and visualized.

Purified protein was treated with peptide:*N*-glycosidase F (PNGase F; Roche Applied Science) at 37 °C with 80 μl of gel filtration buffer, 10 μl of PNGase F, and 130 μg of hAQP10 and mixed to a final volume of 100 μl. After a 5-min incubation, the sample was analyzed on SDS-PAGE and stained with Coomassie. Coomassie-stained SDS-PAGE and immunoblots were analyzed using Multi Gauge V3.0 (Fujifilm) to estimate the intensity of the two bands to estimate the ratio of glycosylated protein by densitometry.

Crystallization—Crystallization attempts using the hanging drop method at 8 °C were performed. For robot setups, a HoneyBee robot (Cartesian) was used with a drop volume of 100 nl + 100 nl whereas for manual setup, a drop size of 1 μl + 1 μl was utilized. Crystals of hAQP10-N133Q appeared after 12 days in condition 2.34 from the MemGold screen (Molecular Dimensions) corresponding to 0.1 M lithium sulfate, 0.1 M glycine, pH 9.3, and 30% v/v PEG400. Crystals could be obtained both in a small drop volume, common for crystallization robots, as well as from larger drop volumes as used in the manual setup.

Circular Dichroism—Circular dichroism (CD) was performed on a Chirascan circular dichroism spectrometer (Applied Photophysics). For the CD spectra measured between 250 and 200 nm, protein samples and a blank containing only buffer was all measured 10 times and averaged with time per point set to 0.5 s. The buffer and the background from the instrument (no sample cuvette in place) were subtracted from the protein trace, and the resulting curve was smoothened (window 3) using the Pro-Data Viewer program accompanying the instrument. Finally, the protein concentration, the path length of the cuvette (0.1 cm), and the mean residue molecular mass (106 Da) were taken into account by converting the

machine units (mdeg) to the mean residue molar ellipticity. For the melting curves, the fixed wavelength 222 nm was used, and time per point was set to 2 s. The temperature was slowly increased by 0.5 °C/min with a tolerance of 0.2 °C starting at 20 °C and ranging to 100 °C.

Functional Studies—Liposomes were formed by dissolving *Escherichia coli* polar lipid extract (Avanti Polar Lipids, Inc.) together with 2% *n*-octyl-β-D-glucopyranoside (Affymetrix) with a lipid to protein ratio of 50 (w/w) in reconstitution buffer (50 mM NaCl, 50 mM Tris-HCl, pH 8.0). Detergent-absorbing polystyrene divinylbenzene beads (Bio-Beads SM2 Adsorbent; Bio-Rad Laboratories) were added, and the samples were incubated under soft agitation overnight. Liposomes were then pelleted (126,800 × *g*, 1 h, 10 °C) and subsequently resuspended to a final concentration of 4 mg/ml.

For water transport measurements with stopped-flow light scattering, the liposome samples were mixed rapidly with hyperosmotic buffer (570 mM sucrose in reconstitution buffer) in a stopped-flow device (μSFM-20, BioLogic Science Instruments), and scattered light intensity was measured at 90° to the excitation beam. Glycerol and erythritol transport were measured by resuspending the liposome pellets in a glycerol/erythritol containing reconstitution buffer matching the osmolality of the 570 mOsm sucrose/reconstitution buffer solution and performing the experiment as above. Obtained data from three traces were merged, normalized, and fitted to a single exponential curve using Kaleidagraph 3.6 (Synergy Software). The radius of the liposomes was determined by dynamic light scattering, and the osmotic water permeability coefficient (Pf, cm/s) was determined as described earlier (25).

Mass Spectrometry—Bands of interest were excised and in-gel digested (26). After reduction and alkylation, gel pieces were dried by vacuum centrifugation and resaturated in 10 μl of chymotrypsin (10 ng/μl; Roche Applied Science) resolved in 25 mM Tris-HCl, pH 7.8, and 10 mM $CaCl_2$. Digestion was performed overnight at 20 °C and quenched by addition of 10 μl of 0.1% trifluoroacetic acid. Peptides were extracted by C18 ziptips (Millipore) according to the manufacturer's protocol, and the eluate was dried by vacuum centrifugation. Dried extracts were resolved in 15 μl of 0.1% formic acid in water and analyzed (27) by LC-MS/MS on a hybrid linear ion-trap orbitrap (LTQ-orbitrap; Thermo Scientific). Spectral data were extracted from the RAW files by using Raw2MSN (28), searches were performed against SwissProt release 2010_06 using MASCOT (2.2.04 Matrixscience). The search parameters were set to 5 ppm MS accuracy, 0.5 Da MS/MS accuracy, enzyme chymotrypsin allowing 2 miss cleavages, fixed modification carbamidomethyl on cystine, and a variable modification of oxidized in methionine. Peptide identifications were accepted if based on a peptide score above 20. Glycan composition and position were determined by manual interpretation of the collision-induced dissociation fragmentation spectra, using the Xcalibur software version 2.1.X (Thermo Scientific).

RESULTS

Human AQP10 is glycosylated in *P. pastoris*. As previously reported, the overproduction yield of hAQP10 in *P. pastoris* is among the highest achieved for any of the human aquaporins (23). After a two-step purification procedure, 30 mg of pure protein/liter of fermentor culture was obtained. However, when analyzed by SDS-PAGE or immunoblotting, recombinant hAQP10 migrates as two bands (Fig. 2*A*) of different molecular masses, implying that there are two forms of the hAQP10 present after purification, presumably due to post-translational modification. To identify the possible modification we used glycoprotein staining, digestion by PNGase F and mass spectrometry analysis.

Glycostaining of hAQP10 showed a more intense signal for the high molecular mass band than for the low molecular mass band (~32 kDa and ~28 kDa, respectively; Fig. 2*B*). In contrast, when stained to indicate the total protein present, the low molecular mass band was stronger (Fig. 2*A*). This finding indicates that the higher molecular mass protein signal contains glycosylated protein yet the majority of the hAQP10 protein is found to be nonglycosylated. This assignment was supported by PNGase F treatment, which specifically cleaves off asparagine-bound glycans to produce ammonia and aspartic acid from asparagine and is one of the most efficient ways to remove a complete *N*-linked glycan. Upon PNGase F treatment the two separated bands were reduced to one band that corresponded to the lower molecular mass signal obtained for the nonglycosylated form of hAQP10 (Fig. 2*C*). Finally, mass spectrometry analysis of both protein samples of different molecular masses showed that the glycosylated form could be detected only in the high molecular mass band.

Human AQP10 has three *N*-linked glycosylation sequons (supplemental Table S1), of which two are projected to the outside of the membrane and hence are possible sites for the glycan to attach. Nevertheless, the peptide found to contain the glycan (TGGNLTVTGPKETASIF) was identified by mass spectrometry (supplemental Table S2), establishing that only asparagine 133 was glycosylated in hAQP10. From the mass of fragments observed with mass spectroscopy analysis and knowing that *P. pastoris* only have glycosyltransferases to use mannose and GlcNAc residues, we could specify the structure of the glycan. The major glycan was thus found to be $Man_9GlcNAc_2$ with some low amounts of $Man_8GlcNAc_2$ (supplemental Fig. S1). The fraction of glycosylated protein was estimated by densitometry analysis of the two signals from several SDS-PAGE and immunoblot gels ($n = 9$), giving that the glycosylated form represents 35% ± 2% of the total hAQP10 population.

Separation of Glycosylated and Nonglycosylated Protein—To separate the two hAQP10 forms, an additional purification step was introduced whereby hAQP10 was bound to a concanavalin A-Sepharose 4B affinity column (GE Healthcare), which binds specifically to mannose- and glucose-containing glycans. In this manner nonglycosylated hAQP10 (hAQP10-ΔGlyc) was collected while the glycosylated protein remained bound to the column. A surprising result was that ~70% of the protein loaded could not be eluted from the column even though only 35% of the protein appeared to be glycosylated. This observation may be because the majority of AQP tetramers containing at least one glycosylated protomer bound strongly to the column, although strong hydrophobic interactions between detergent-solubilized protein and the column media also interfere

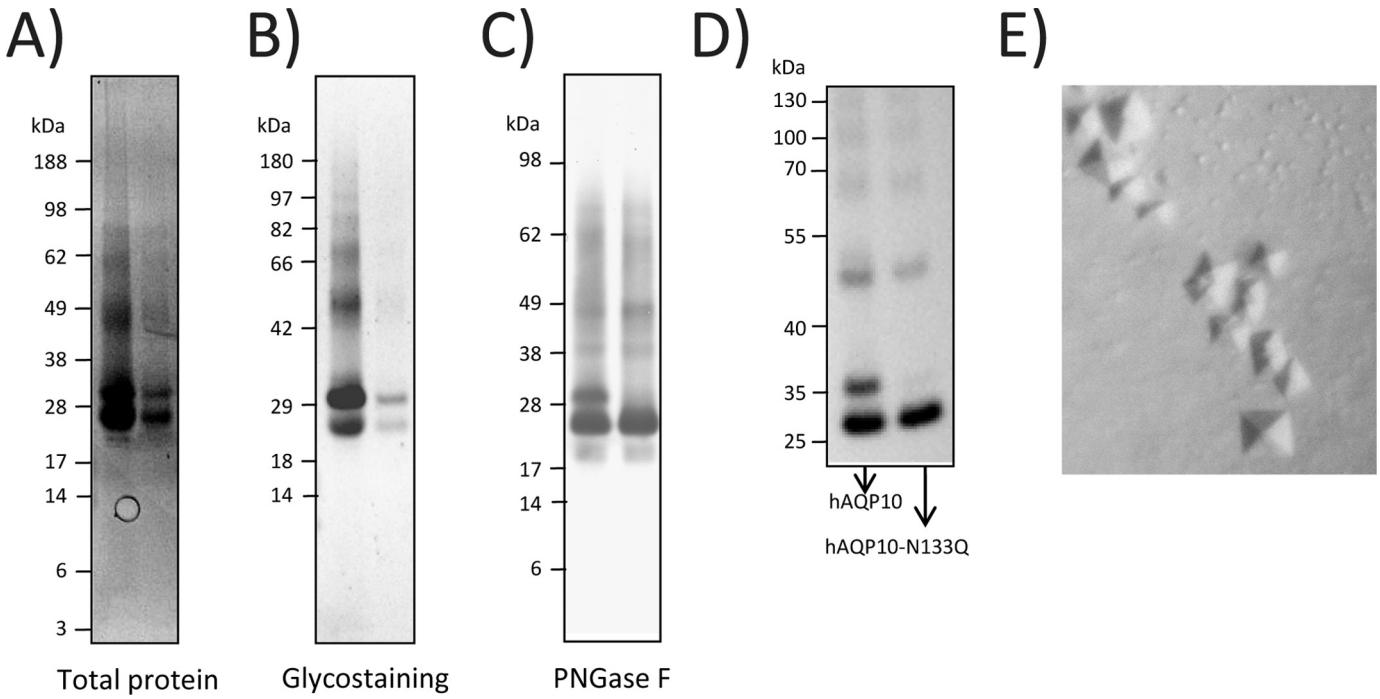

FIGURE 2. *A*, SDS-PAGE of hAQP10 stained with Pro SYPRO Ruby, which stains all proteins. *B*, SDS-PAGE -of hAQP10 stained with Pro-Q Emerald 488 glycoprotein gel stain, indicating fragments containing glycosylated protein. For *A* and *B*, 1 μg and 100 ng of protein have been loaded, respectively; the highest is in the *leftmost lane* followed by a 10 times dilution in the following *lane*. The larger fragment (*upper band*) is the glycosylated population. *C*, SDS-PAGE of hAQP10 stained with Fairbanks Coomassie stain. The *left lane* shows the sample prior to PNGase F treatment and the *right lane* the result, which clearly shows how the glycan has been digested by the enzyme. *D*, immunoblot showing hAQP10 and hAQP10-N133Q where the latter gives a homogeneous sample suitable for crystallization setups. The primary and secondary antibodies are Clontech His_6 monoclonal antibody and Promega anti-mouse IgG HRP conjugate, respectively. *E*, using the hanging drop method at 8 °C small crystals formed for hAQP10-N133Q in condition 2.34 from the MemGold screen (Molecular Dimensions) corresponding to 0.1 M lithium sulfate, 0.1 M glycine, pH 9.3, and 30% v/v PEG400.

with the binding. Eluted protein was analyzed with mass spectrometry, and no glycosylated population was observed.

An efficient way to remove glycans is to apply site-directed mutagenesis, with the asparagine to glutamine mutation being the most popular choice to disrupt the *N*-linked glycosylation sequon (29). We thus overproduced hAQP10 with asparagine 133 mutated to a glutamine (Fig. 1), and the resulting mutant protein (hAQP10-N133Q) migrated as a single band with the same molecular mass as the nonglycosylated form of hAQP10 (Fig. 2*D*). Interestingly, compared with the wild-type protein, the N133Q hAQP10 mutant yielded crystals (Fig. 2*E*) diffracting to low resolution. This observation is most likely related to the enrichment of a highly homogeneous sample. We have solved the x-ray structures of three eukaryotic aquaporins using protein overproduced in *P. pastoris* (30, 31), and it is apparent that hAQP10-N133Q is a promising candidate for further structural studies.

Human AQP10 Transports Water, Glycerol, and Other Sugar Alcohols—Purified protein was inserted into liposomes (creating proteoliposomes), and water, glycerol, and erythritol transport activity was assayed using stopped-flow light scattering, for which a shrinkage in hypertonic solution is observed and compared with control liposomes lacking protein (Fig. 3). All of the hAQP10 variants assayed (hAQP10, hAQP10-ΔGlyc, and hAQP10-N133Q) showed similar facilitated transport of water, glycerol ($C_3H_5(OH)_3$), and erythritol ($C_4H_6(OH)_4$). The measured rate constants were ~1000:100:1 for water:glycerol:erythritol, respectively (Table 1). The calculated Pf value for the hAQP10 (hAQP10-N133Q) water transport was estimated to 7.3 ± 0.02 compared with the control, 2.4 ± 0.01.

The transport rate for hAQP10-N133Q was slower than the observed rate for the other forms of hAQP10. Although the reason behind this is not clear, a single mutation has been reported to affect the transport rate in another case for the sole aquaporin of the parasite *Plasmodium falciparum* (PfAQP) (32).

Rapid stopped-flow transport assays were complemented using a surface plasmon resonance (SPR)-based assay (33) (see also supplemental Experimental Procedures). Compared with stopped-flow based measurements, this SPR based assay is advantageous for measuring the slower transport of larger molecules such as xylitol ($C_5H_7(OH)_5$) as was verified in studies on a related aquaglyceroporin (33). Supplemental Fig. S2 shows time-dependent SPR traces recorded from immobilized proteoliposomes. These traces are characterized by two kinetic components: a slow component corresponding to the passive diffusion over empty liposome (*i.e.* no hAQP10 inserted) and a fast component representing facilitated transport by hAQP10 (supplemental Fig. S2). In fitting these data, a single exponential curve was optimized to the traces between 16 and 100 s (supplemental Table S3, Single exp), and a double exponential curve was fitted to the fast component (shown in supplemental Fig. S2 *insets*), yielding both the slower rate constant for the passive diffusion as well as the rate constant for the transport (supplemental Table S3, Double exp). The rate constant were ~2:1 for erythritol:xylitol transport, respec-

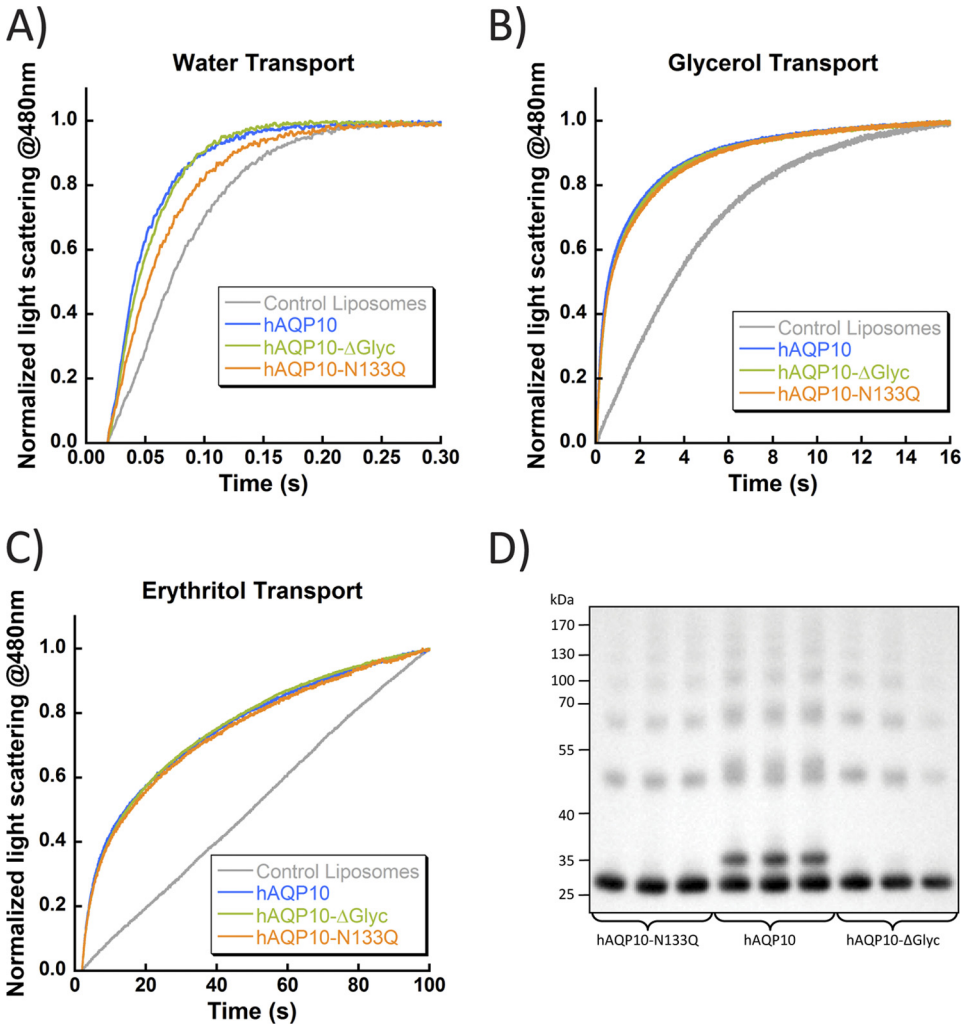

FIGURE 3. **Functional analysis of hAQP10 reconstituted into proteoliposomes using stopped-flow light scattering.** *A–C*, trace for proteoliposomes containing wild type hAQP10 in *blue*, hAQP10-ΔGlyc in *green*, hAQP10-N133Q in *orange*, and control liposomes lacking protein in *gray* ($n = 3$). The plots show transport of water (*A*), glycerol (*B*), and erythritol (*C*). *D*, immunoblot showing triplicate protein samples used in stopped-flow light scattering for water, glycerol, and erythritol transport, respectively. The samples used for water transport were also used for SPR measurements with Biacore.

TABLE 1

Rate constants for transport of water, glycerol, and erythritol

A single exponential curve was fitted to the three averaged stopped-flow light scattering data (shown in Fig. 3), and the rate constants ± S.E. are listed for the transport of different molecules. The goodness of the curve fit is given as the coefficient of determination, R^2.

Protein	Rate constant	R^2
	s^{-1}	
Water transport		
Control liposomes	15 ± 0.11	0.995
hAQP10	31 ± 0.09	0.998
hAQP10-ΔGlyc	29 ± 0.09	0.999
hAQP10-N133Q	21 ± 0.06	0.999
Glycerol transport		
Control liposomes	0.20 ± 0.0002	0.999
hAQP10	0.54 ± 0.002	0.966
hAQP10-ΔGlyc	0.55 ± 0.002	0.970
hAQP10-N133Q	0.49 ± 0.002	0.972
Erythritol transport		
Control liposomes	0.0053 ± 0.0002	0.996
hAQP10	0.030 ± 0.0004	0.983
hAQP10-ΔGlyc	0.032 ± 0.0004	0.999
hAQP10-N133Q	0.029 ± 0.0004	0.986

tively. From these results we conclude that molecules larger than glycerol pass through the aquaglyceroporin, however at a lower transport rate.

Glycosylation of hAQP10 Increases Thermostability—CD is a useful low resolution technique to examine protein structure in solution. In particular, it can be used to address differences in secondary structure between native and recombinant protein as well as differences between wild-type and mutant proteins (34). To investigate the effect of glycosylation, CD studies were made on native protein (hAQP10), mutated protein (hAQP10-N133Q) lacking the possibility to acquire a glycan, and on non-glycosylated protein (hAQP10-ΔGlyc) isolated by an additional purification step described above. Measurements over the far UV domain (200–250 nm) are typically performed for secondary structure studies of membrane proteins because several components of a membrane protein buffer, such as salt and detergent, interfere and absorb at wavelengths under 200 nm (35). Thus, our scans from 250 to 200 nm avoided high absorption artifacts yet covered the largest feature associated with α-helices at 208 and 222 nm.

Fig. 4*A* shows the results of CD analysis. It is apparent that the secondary structure content is the same for all forms of hAQP10 because there is strong overlap of all CD traces. Moreover, the α-helical content can be estimated from the mean

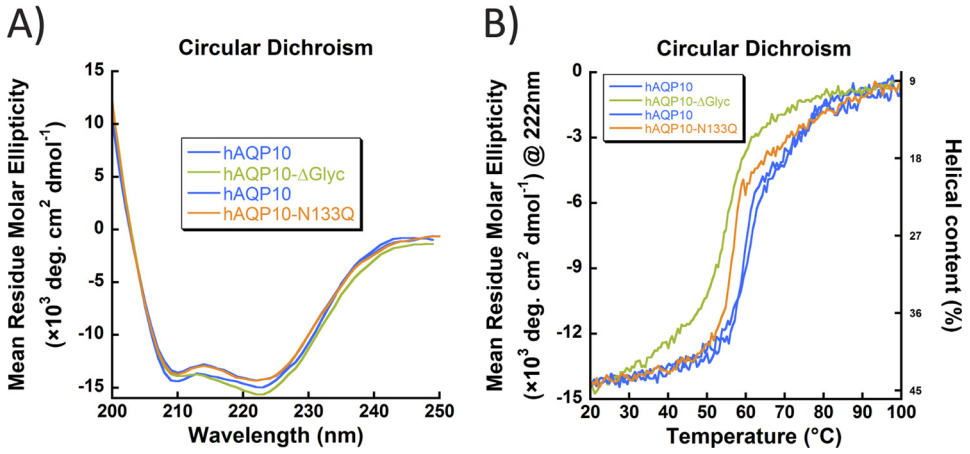

FIGURE 4. **CD spectra and melting curves, demonstrating the stability of hAQP10.** *Traces* for wild-type hAQP10 are marked in *blue*, hAQP10-ΔGlyc in *green*, hAQP10-N133Q in *orange*. The hAQP10 samples are from the same preparation. *A*, spectra showing the content of secondary structure in various forms of hAQP10. *B*, melting curves representing thermostability of the protein.

residue molar ellipticity ([θ] value at 222 nm (36) using the formula ([θ] − 3000)/(−36000 − 3000). Because $[\theta]_{222} \approx -14500$ for all samples this gives an approximate α-helical content of 45%, which is consistent with the observed value for hAQP1 (37). Thus, CD analysis demonstrates that the secondary structure of the proteins is similar, suggesting a similar tertiary structure and a correctly folded protein. Neither, the glycan nor the mutation alters the basic protein fold.

CD is an excellent tool to study protein folding and/or unfolding as a function of temperature or in the presence of denaturing agents. Loss of CD signal can be observed over time, providing information about the stability of the protein (38), or by gradually increasing the temperature while monitoring the signal at 222 nm, which yields a measurement of the protein thermostability quoted as the apparent melting temperature (T_m) of the protein. Melting curves measured from all three AQP10 variants showed that the α-helical content dropped from the initial value of 45% at 20 °C to 9% at 100 °C and revealed a significant impact of glycosylation on the protein thermal stability (Fig. 4*B*). For two independent measurements on glycosylated hAQP10 we obtained apparent melting temperatures T_m = 60.9 °C and T_m = 59.5 °C; for the nonglycosylated hAQP10-N133Q mutant T_m = 56.6 °C; and for the nonglycosylated hAQP10-ΔGlyc T_m = 55.0 °C (Table 2 and supplemental Fig. S3). This significant shift in melting temperature of 3 to 6 °C suggests that the glycosylation has a stabilizing role in the proteins native environment.

TABLE 2

Apparent melting temperatures (T_m) for all forms of hAQP10 in this study

A single lorentzian function was fitted to the derived curves, and the center ± S.E. in the table and as a dotted black curve (supplemental Fig. S3). The goodness of fit curve is given as the coefficient of determination, R^2.

Protein	Apparent T_m	R^2
	℃	
hAQP10	60.9 ± 0.20	0.738
hAQP10-ΔGlyc	55.0 ± 0.20	0.808
hAQP10	59.5 ± 0.14	0.755
hAQP10-N133Q	56.6 ± 0.09	0.832

DISCUSSION

One striking distinction between aquaporins that transport glycerol (aquaglyceroporins) and the orthodox water transporters is that the aquaglyceroporins typically have a significantly extended C-loop (39) (supplemental Table S4). In this respect it is noteworthy that the C-loop of hAQP10 is the longest of the human aquaporins, and its length is comparable with that of the *E. coli* glycerol uptake facilitator protein GlpF (40). Our work confirms previous observations of glycerol transport activity for AQP10 (3) and further demonstrates that hAQP10 facilitates the membrane transport of longer sugar alcohols such as erythritol and xylitol. Erythritol is used as a low calorie sweetener and is about 70% as sweet as sugar (sucrose). Most ingested erythritol is absorbed in the small intestine, and, consequently, erythritol does not induce a laxative effect as has been observed for other sugar alcohols such as sorbitol (41). From this basis the observed transport of erythritol transport reported here suggests a plausible absorbing function for hAQP10 *in vivo*.

It has been observed that some of the aquaglyceroporins also have significant water transport activity, such as the sole aquaporin of the parasite *P. falciparum* (PfAQP) (42), whereas others have very limited water transport activity, such as GlpF of *E. coli* (43) for which another aquaporin (AQPZ) facilitates water transport. When assayed in *Xenopus* oocytes, hAQP10 was reported to be primarily a glycerol transporter with limited water transport (2, 3). In contrast, our work in proteoliposomes clearly shows a high intrinsic water transport activity for hAQP10 that was comparable with that obtained for other pure water transporters such as hAQP1; Pf = 9.1 ± 0.4 (control: 3.1 ± 0.01) (25) and hAQP4; Pf = 7.5 ± 0.03 (control: 2.4 ± 0.01).[3] Very significant differences in the apparent water transport activity were also obtained for the sole aquaporin of *P. pastoris* (AQY1) when measured in native membranes (spheroplasts) or when reconstituted into proteoliposomes (44). For the case of AQY1, its crystal structure revealed that the water channel was regulated by gating (45), and it was suggested that reconstitution of AQY1 into proteoliposomes, which have a

[3] F. Öberg, J. Sjöhamn, G. Fischer, A. Moberg, A. Pedersen, R. Neutze, and K. Hedfalk, unpublished work.

different lipid content and curvature than the *P. pastoris* plasma membrane, may have activated AQY1 due to mechanosensitivity (44). It is unclear whether a similar mechanism could regulate the functional activity of hAQP10 and thereby reconcile these apparently contradictory water transport measurements in proteoliposomes and oocytes.

Although several human aquaporins are predicted to have *N*-linked glycosylation (TMHMM Server v.2.0) (supplemental Table S1) it is significant that hAQP10 is the only human aquaporin to be glycosylated when overproduced in *P. pastoris*. Because *N*-linked glycosylation is initiated in the ER lumen, only the extracellular side of the functional protein will be accessible for this type of modification. In humans, hAQP1 is known to be glycosylated (47), but this has not been observed in *P. pastoris* (23). As such it appears that the *P. pastoris* machinery is less prone to form *N*-linked glycans than a human cell. A typical epithelial cell, such as the cells in the small intestine where hAQP10 is located, is polarized with an apical domain facing the lumen, and the remainder of the cell is termed the basolateral domain. To keep the two domains separate the protein sorting mechanisms in the Golgi apparatus target protein to different locations. Membrane proteins destined for the basolateral domain have signal sequences whereas those targeted for the apical membrane can be flagged by the presence of a glycosylphosphatidylinositol anchor (48), specific membrane-spanning regions (49), and *N*-glycans (16, 17). It has been reported that hAQP10 is the only aquaporin found in the apical domain in the human small intestine (5), and it seems likely the *N*-linked glycan directs it to the apical membrane, as has been shown for the human organic anion transporter for which the glycan was found to be essential for proper trafficking (50). In addition to a possible role in trafficking, it is noteworthy that the absorptive epithelial cells in the human small intestine are covered by a cell coat called the glycocalyx which is composed of oligosaccharide side chains of the glycolipid and glycoprotein components of the membrane (51). Together with the thicker mucus layer, this cell coat serves as a barrier against pathogens and toxins and regulates access to the apical membranes (52). The *N*-linked glycan found in hAQP10 could also form a part of the glycocalyx (53, 54), indicating another functional role for hAQP10 glycosylation.

A stabilizing effect of glycosylation has been reported for other membrane transporters such as AQP2 mutants (55) and a shaker potassium channel (56). The temperature dependence of the CD analysis indicates that the wild-type population (with 35% glycosylated and 65% nonglycosylated) and the hAQP10-N133Q population (100% nonglycosylated) show very similarly shaped temperature-dependent curves but shifted by 3–6 °C. Moreover, the very small yield of glycan-free hAQP10 that was eluted from the concanavalin A-Sepharose 4B affinity column (hAQP10-ΔGlyc) was even less stable than both the hAQP10-N133Q and the wild-type construct. The magnitude of the stabilization for wild-type hAQP10 is in good agreement with reported increases in apparent T_m for globular proteins glycosylated at single sites (57, 58). Together, these results demonstrate that an increased thermal stability is imparted to hAQP10 by glycosylation.

A possible interpretation of the data is that the presence of at least one glycosylated hAQP10 within the tetramer is necessary and sufficient to convey an enhanced temperature stability of 3–6 °C. If the number of *N*-glycosylated proteins/tetramer were randomly distributed, then only 18% (0.65^4) of the aquaporin tetramers would not contain any *N*-glycosylation. In reality, however, the fraction of nonglycosylated tetramers is likely to be even smaller due to steric effects preventing the presence of multiple glycans within a single tetramer, as observed for hAQP1 where only one protomer/tetramer was found to be glycosylated in the human body (47). This argument implies that the overwhelming majority of tetramers in the hAQP10 wild-type sample contain at least one glycosylated protein, explaining why the CD titration with temperature indicates only one well behaved population with enhanced thermal stability. Conversely, from this argument we are led to conclude that the presence of a single glycosylation within the tetramer is sufficient to convey the full 3–6 °C enhanced stability to the other closely packed protomers, suggesting a novel cooperative mechanism of glycan-enhanced thermostability. Although this conclusion is somewhat intuitive, given the close packing and relatively high stability of aquaporins, it also seems reasonable to expect that this cooperative thermostability effect would be generic. Given that almost all integral membrane proteins form oligomers and many are glycosylated, we anticipate that a mechanism of enhanced glycan thermostability conveyed through cooperative interactions within the oligomer may be a rather widespread mechanism of membrane protein stabilization throughout biology.

Acknowledgments—We thank Louise Fornander for assistance and guidance at the circular dichroism spectrometer and Sjoerd van der Post for help with mass spectrometry analysis.

REFERENCES

1. King, L. S., Kozono, D., and Agre, P. (2004) *Nat. Rev. Mol. Cell Biol.* **5,** 687–698
2. Hatakeyama, S., Yoshida, Y., Tani, T., Koyama, Y., Nihei, K., Ohshiro, K., Kamiie, J. I., Yaoita, E., Suda, T., Hatakeyama, K., and Yamamoto, T. (2001) *Biochem. Biophys. Res. Commun.* **287,** 814–819
3. Ishibashi, K., Morinaga, T., Kuwahara, M., Sasaki, S., and Imai, M. (2002) *Biochim. Biophys. Acta* **1576,** 335–340
4. Li, H., Kamiie, J., Morishita, Y., Yoshida, Y., Yaoita, E., Ishibashi, K., and Yamamoto, T. (2005) *Biol. Cell* **97,** 823–829
5. Mobasheri, A., Shakibaei, M., and Marples, D. (2004) *Histochem. Cell Biol.* **121,** 463–471
6. Lis, H., and Sharon, N. (1993) *Eur. J. Biochem.* **218,** 1–27
7. Apweiler, R., Hermjakob, H., and Sharon, N. (1999) *Biochim. Biophys. Acta* **1473,** 4–8
8. Marshall, R. D. (1974) *Biochem. Soc. Symp.* 17–26
9. Atkinson, P. H., and Lee, J. T. (1984) *J. Cell Biol.* **98,** 2245–2249
10. Jamieson, J. D., and Palade, G. E. (1968) *J. Cell Biol.* **39,** 589–603
11. Gemmill, T. R., and Trimble, R. B. (1999) *Biochim. Biophys. Acta* **1426,** 227–237
12. Hamilton, S. R., Bobrowicz, P., Bobrowicz, B., Davidson, R. C., Li, H., Mitchell, T., Nett, J. H., Rausch, S., Stadheim, T. A., Wischnewski, H., Wildt, S., and Gerngross, T. U. (2003) *Science* **301,** 1244–1246
13. Grinna, L. S., and Tschopp, J. F. (1989) *Yeast* **5,** 107–115
14. Trimble, R. B., Atkinson, P. H., Tschopp, J. F., Townsend, R. R., and Maley, F. (1991) *J. Biol. Chem.* **266,** 22807–22817
15. Sato, Y., and Endo, T. (2010) *Geriatr. Gerontol. Int.* **101,** S32–40

16. Scheiffele, P., Peränen, J., and Simons, K. (1995) *Nature* **378,** 96–98
17. Keller, P., and Simons, K. (1997) *J. Cell Sci.* **110,** 3001–3009
18. Elbein, A. D. (1991) *Trends Biotechnol.* **9,** 346–352
19. Voet, D., and Voet, J. G. (2004) *Biochemistry*, 3rd Ed., pp. 369–379, J. Wiley & Sons, New York
20. Nakagawa, H., Wakabayashi-Nakao, K., Tamura, A., Toyoda, Y., Koshiba, S., and Ishikawa, T. (2009) *FEBS J.* **276,** 7237–7252
21. Gong, Q., Anderson, C. L., January, C. T., and Zhou, Z. (2002) *Am. J. Physiol. Heart Circ. Physiol.* **283,** H77–84
22. Shental-Bechor, D., and Levy, Y. (2008) *Proc. Natl. Acad. Sci. U.S.A.* **105,** 8256–8261
23. Oberg, F., Ekvall, M., Nyblom, M., Backmark, A., Neutze, R., and Hedfalk, K. (2009) *Mol. Membr. Biol.* **26,** 215–227
24. Invitrogen (2002) *Pichia Fermentation Process Guidelines*, Invitrogen, Carlsbad, CA
25. Nyblom, M., Oberg, F., Lindkvist-Petersson, K., Hallgren, K., Findlay, H., Wikström, J., Karlsson, A., Hansson, O., Booth, P. J., Bill, R. M., Neutze, R., and Hedfalk, K. (2007) *Protein Expr. Purif.* **56,** 110–120
26. Shevchenko, A., Tomas, H., Havlis, J., Olsen, J. V., and Mann, M. (2006) *Nat. Protoc.* **1,** 2856–2860
27. Johansson, M. E., Thomsson, K. A., and Hansson, G. C. (2009) *J. Proteome Res.* **8,** 3549–3557
28. Olsen, J. V., de Godoy, L. M., Li, G., Macek, B., Mortensen, P., Pesch, R., Makarov, A., Lange, O., Horning, S., and Mann, M. (2005) *Mol. Cell Proteomics* **4,** 2010–2021
29. Iyengar, R., and Hildebrandt, J. D. (2002) *Methods in Enzymology*, Vol. 343, *G Protein Pathways, P. A., Receptors*, p. 205, Academic Press, New York
30. Horsefield, R., Nordén, K., Fellert, M., Backmark, A., Törnroth-Horsefield, S., Terwisscha van Scheltinga, A. C., Kvassman, J., Kjellbom, P., Johanson, U., and Neutze, R. (2008) *Proc. Natl. Acad. Sci. U.S.A.* **105,** 13327–13332
31. Törnroth-Horsefield, S., Wang, Y., Hedfalk, K., Johanson, U., Karlsson, M., Tajkhorshid, E., Neutze, R., and Kjellbom, P. (2006) *Nature* **439,** 688–694
32. Beitz, E., Pavlovic-Djuranovic, S., Yasui, M., Agre, P., and Schultz, J. E. (2004) *Proc. Natl. Acad. Sci. U.S.A.* **101,** 1153–1158
33. Brändén, M., Tabaei, S. R., Fischer, G., Neutze, R., and Höök, F. (2010) *Biophys. J.* **99,** 124–133
34. Kelly, S. M., Jess, T. J., and Price, N. C. (2005) *Biochim. Biophys. Acta* **1751,** 119–139
35. Creighton, T. E. (1997) *Protein Structure: A Practical Approach*, 2nd Ed., pp. 268–269, IRL, Oxford, New York
36. Morrisett, J. D., David, J. S., Pownall, H. J., and Gotto, A. M., Jr. (1973) *Biochemistry* **12,** 1290–1299
37. Sui, H., Han, B. G., Lee, J. K., Walian, P., and Jap, B. K. (2001) *Nature* **414,** 872–878
38. Greenfield, N. J. (2006) *Nat. Protoc.* **1,** 2527–2535
39. Tusnády, G. E., and Simon, I. (2001) *Bioinformatics* **17,** 849–850
40. Fu, D., Libson, A., Miercke, L. J., Weitzman, C., Nollert, P., Krucinski, J., and Stroud, R. M. (2000) *Science* **290,** 481–486
41. Munro, I. C., Berndt, W. O., Borzelleca, J. F., Flamm, G., Lynch, B. S., Kennepohl, E., Bär, E. A., and Modderman, J. (1998) *Food Chem. Toxicol.* **36,** 1139–1174
42. Newby, Z. E., O'Connell, J., 3rd, Robles-Colmenares, Y., Khademi, S., Miercke, L. J., and Stroud, R. M. (2008) *Nat. Struct. Mol. Biol.* **15,** 619–625
43. Borgnia, M. J., and Agre, P. (2001) *Proc. Natl. Acad. Sci. U.S.A.* **98,** 2888–2893
44. Fischer, G., Kosinska-Eriksson, U., Aponte-Santamaría, C., Palmgren, M., Geijer, C., Hedfalk, K., Hohmann, S., de Groot, B. L., Neutze, R., and Lindkvist-Petersson, K. (2009) *PLoS Biol.* **7,** e1000130
45. Törnroth-Horsefield, S., Hedfalk, K., Fischer, G., Lindkvist-Petersson, K., and Neutze, R. (2010) *FEBS Lett.* **584,** 2580–2588
46. Deleted in proof
47. Heymann, J. B., Agre, P., and Engel, A. (1998) *J. Struct. Biol.* **121,** 191–206
48. Lisanti, M. P., Le Bivic, A., Saltiel, A. R., and Rodriguez-Boulan, E. (1990) *J. Membr. Biol.* **113,** 155–167
49. Kundu, A., Avalos, R. T., Sanderson, C. M., and Nayak, D. P. (1996) *J. Virol.* **70,** 6508–6515
50. Zhou, F., Xu, W., Hong, M., Pan, Z., Sinko, P. J., Ma, J., and You, G. (2005) *Mol. Pharmacol.* **67,** 868–876
51. Ito, S. (1974) *Philos, Trans. R Soc. Lond. B Biol. Sci.* **268,** 55–66
52. Mestecky, J. (2005) *Mucosal Immunology* (Mestecky, J., Ogra, P. L., McGhee, J. R., Lambrecht, B. N., and Strober, W., eds) 3rd Ed., Elsevier, Amsterdam
53. Frey, A., Giannasca, K. T., Weltzin, R., Giannasca, P. J., Reggio, H., Lencer, W. I., and Neutra, M. R. (1996) *J. Exp. Med.* **184,** 1045–1059
54. Ishimura, K., Kurihara, H., and Fujita, H. (1984) *Cell Tissue Res.* **238,** 653–656
55. Buck, T. M., Eledge, J., and Skach, W. R. (2004) *Am. J. Physiol. Cell Physiol* **287,** C1292–1299
56. Khanna, R., Myers, M. P., Lainé, M., and Papazian, D. M. (2001) *J. Biol. Chem.* **276,** 34028–34034
57. Wang, C., Eufemi, M., Turano, C., and Giartosio, A. (1996) *Biochemistry* **35,** 7299–7307
58. Pfeil, W. (2002) *Thermochim. Acta* **382,** 169–174